

Seismic Noise Attenuation Using Curvelet Transform and Dip Map Data Structure

T. Nguyen* (PGS), Y.J. Liu (PGS)

Summary

The curvelet transform is a known tool used in the attenuation of coherent and incoherent noise in seismic data. It utilises the fact that signal and noise are usually better separated in the curvelet domain than in the time-space (TX) domain. Coefficients of the transform are not independent and neighbouring coefficients are strongly correlated, which existing curvelet-based noise attenuation algorithms do not fully utilise. In this work we propose to use a data structure called a 'dip map' to describe dip information in seismic data. This information links local curvelet coefficients together in adaptive thresholding or subtraction of curvelet coefficients in seismic denoising algorithms. We used the dip map to improve curvelet multiple subtraction algorithm and the results show significant improvement over traditional methods with real data.

Introduction

All acquired seismic data are contaminated by noises that need to be removed or attenuated before further processing and interpretation can take place. The methods for seismic data denoising can be broadly classified into prediction filter methods and transform-based methods. In this paper we continue previous works on seismic data denoising using curvelet transform by using a technique that connects transform domain curvelet coefficients to seismic events in the original time-space (TX) domain.

Curvelet transform has been used successfully in seismic denoising of both incoherent and coherent noise (Neelamani et al., 2008) mainly because of useful properties that can be leveraged: 1. Curvelets provide a sparse representation of seismic events, 2. events of differing dip, scale or TX location will often be well separated in the curvelet domain. The curvelet transform represents any 2D image as a linear sum of curvelet dictionary functions weighted by corresponding coefficient values. The data is decomposed into multiple scales, with each scale divided equally into multiple directions. Curvelet basis functions are designed to be simultaneously localized in scale, direction, space and time. Each curvelet coefficient is thus identified by a multi-index consisting of scale, direction and space-time indices. Each scale-direction (curvelet subband) is strictly band-limited, hence each curvelet subband is decimated to a much smaller size when compared to the original data (Nguyen et al., 2010).

An example of the amplitude of complex curvelet domain coefficients is illustrated in Figure 1 (left). Each coefficient $C(i,j,t,x)$ has scale index i , direction index j , and time-space indices t,x . Figure 1 (right) also illustrates the relationship between neighboring coefficients: coefficients with the same (j,t,x) describe the same event, but at different frequencies (or scale), group of coefficients at the same curvelet subband (i,j) describe linear seismic events, and coefficients with the same (i,t,x) describe events whose directions fall between multiple curvelet bands. The coefficients having close scale-direction-location indices in the curvelet domain are strongly correlated, because they describe approximately the same seismic events. Therefore our aim is to have a data structure to link neighboring curvelet coefficients in noise attenuation algorithms based on geometrical characteristics of seismic events in TX domain.

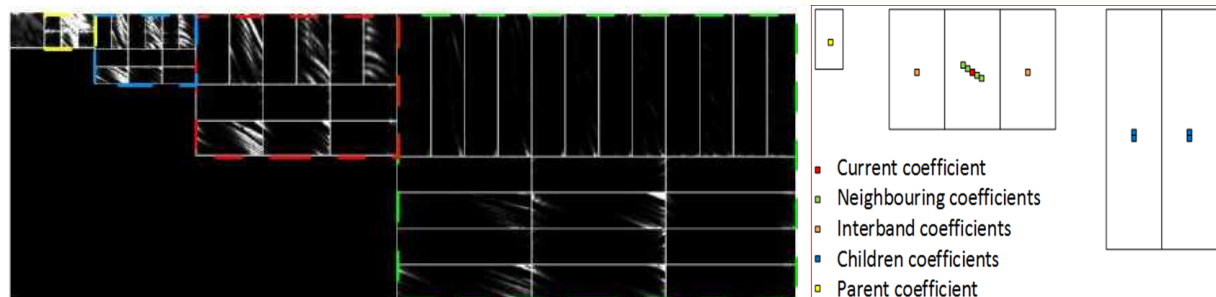


Figure 1 Left: an example of complex curvelet representation of a typical seismic shot gather with primary and multiple noise, and, Right: an example of the relationship of a coefficient with its neighbouring coefficients.

Curvelet transform and the dip map data structure

The dip map is a data structure created for the purpose of connecting seismic events in TX domain to coefficients in transform domain. For a normal 2D TX seismic section the dip map is a 3D data cube $D(t,x,d)$ of time, space and dip dimensions calculated from the data. For each location of the TX data the dip map provides a dip spectrum vector that corresponds to seismic events at that location. Because the objective of the dip map is to provide dip information for the curvelet transform, and the number of curvelet band for each scale is increasing with scale level, the number of dips in the dip map is set equal to the number of curvelet direction at the highest scale.

Seismic data contain continuous and locally linear events; there are continuities between dip map sections corresponding to different times that are close to each other. This is illustrated in Figure 2. The two synthetic events have nearly the same dip at three different times. The dip map sections of time t_0 and t_2 show two separate seismic events in its directions and location, but it is difficult to separate the two events in the dip map section at time t_1 because the two events have the same x

location. At time t_1 the dip map sections from time t_0 and t_2 can help in separating these two crossing events. In practical seismic processing applications using curvelet transform and dip maps, any algorithm will need to estimate dip maps for the signal component and/or dip map for the noise component in case of coherent noise.

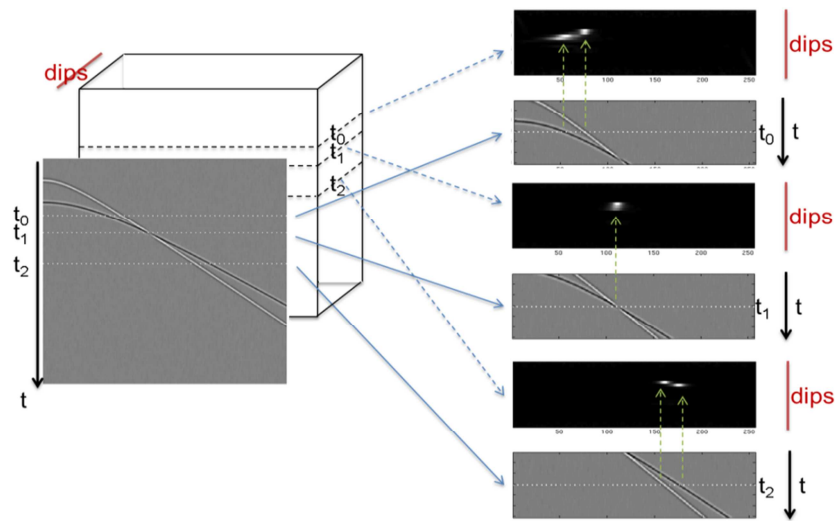


Figure 2 Examples of dip map calculated from a TX section, and three slices in time of the dip map cube correspond to three time location t_0 , t_1 and t_2 .

Application of dip maps to multiple subtraction

We now describe how the dip map was used for our curvelet-domain adaptive multiple subtraction where the amount of rotation and scaling are controlled by an analysis step (Nguyen et al., 2016). A typical approach for adaptive multiple subtraction in the curvelet domain is to rotate and scale each curvelet domain coefficient of the model to match the data coefficient at the same index (Neelamani et al., 2010). The problem of this approach is that it relies on the assumption that primaries and multiples are mapping to different coefficients in the curvelet domain. While it is true that primaries and multiples are better separated in the curvelet domain than in the TX domain, crossing primaries and multiples can be mapped to the same curvelet coefficients. When the multiple model coefficients are rotated and scaled to match the data coefficients, they are not only adapted to the true multiple but also to the primary component, potentially leading to primary damage.

Our algorithm for multiple subtraction (Nguyen et al., 2016) in the curvelet domain consists of an analysis and subtraction phases. The analysis phase takes into account a group of nearby curvelet coefficients estimating the constraint parameters for each pair of curvelet coefficients. These parameters control the amount of adaptation that the curvelet coefficients of the model are allowed to adapt to the data coefficient in the subtraction phase. By considering a group of coefficients together, the analysis phase can match modelled multiples to real multiple events in the TX domain, estimating the suitable adaptation parameter for the corresponding curvelet domain coefficients. Calculating the parameters in the analysis phase requires an estimation of the dip map of the multiple and primary components of the data, step by step as follows:

1. The multiple model is matched to real multiple by LSF (Least Square Filtering).
2. The multiple dip map is estimated from the adapted model (D_M).
3. The multiple is subtracted from the data by curvelet matching with a high level of adaptation.
4. Primary dip map (D_P) is estimated from an over-adapted subtraction with primary damages.
5. A new primary dip map (D_P) is interpolated using the multiple dip map D_M as a weighting mask to compensate for multiple masking of primary events.

In step 3, the multiple is subtracted with high adaptation parameters to ensure all multiples are subtracted and the result contains only primary. The crucial part of the analysis phase is to estimate a primary dip map from an over-adapted subtraction with primary damages in step 4. This is done by using the property that dip map events are continuous and linear and using the dip map of the multiple

as a weighting mechanism to compensate for primary events that are masked by multiples. An example of a processing algorithm for primary map reconstruction in step 5 is shown as follows:

- I. Estimate a normalized mask from the multiple dip map $D_M(t,x,d)$ ranging from 0 to 1. For

$$\text{example } \mathbf{M}(t, x, d) = \frac{D_M(t,x,d)}{\max D_M(t,x,d)}$$

- II. For each point (t,x,d) of the dip map of the primary $D_P(t,x,d)$, estimate a new value taking into account the neighbouring value:

$$D_P(t, x, d) = (1 - M(t, x, d))D_P(t, x, d) + M(t, x, d) \sum_{t_i, x_j} W(t_i, x_j, d) D_P(t - t_i, x - x_j, d)$$

where $W(t_i, x_j, d)$ is an anisotropic smoothing window with its main axis in the direction of the current dip d , its value is estimated from $1 - M(t_i, x_j, d)$ and is normalized so that it sums up to 1. The main idea is that when the value of the multiple mask is high, the value of the primary dip map is compensated by taking into account its value further along the direction of the dip.

After the above processing the analysis phase will have estimated dip maps for the primary and multiple components and these can be used to control adaptation level in the subtraction phase. Using the location (t,x) and direction (j) indices of each curvelet coefficient, the dip maps can provide an estimation of the primary and multiple components. The ratio between multiple and primary dip information will control the level of scaling and rotation of the modelled coefficient to match the data before being subtracted. If the amplitude of the multiple dip map is stronger than the primary dip map, the level of adaptation is higher; conversely, if the primary dip map is stronger, the level of adaptation can be reduced. By this way, the primary events are better preserved while high level of curvelet adaptation will remove more residual multiple in weak primary areas.

Examples

The authors have implemented and tested successfully the above algorithm on a synthetic dataset and a real deep water dataset. We present here the result of a test performed on a very challenging shallow water broadband data from the Barents Sea acquired using dual-sensor towed streamer technology. Figure 3 is the stack of the result of conventional model based denoising from which we can see that most of the multiples are attenuated although there is still some visible residual multiple noise left in the region where primaries overlap with complex structure/faults. This residual multiple noise is further attenuated using our new curvelet denoising method (Figures 4,5 and 6).

Because curvelet adaptive subtraction relies on the directionality of the transform and curvelets have a higher number of curvelet directions at higher scales, our method tends to work best at frequencies above 20Hz. We found that at lower frequencies, the improved method for LSF subtraction produces better results. Both multiple subtraction techniques have been integrated into an intelligent adaptive subtraction program (Perrier et al., 2017) that combines different multiple subtraction techniques to produce the optimum demultiple.

Conclusions

The advantage for seismic noise attenuation in the curvelet domain is that noise and signal are better separated in the transform domain. However they are not totally separated and denoising algorithms need to take into account nearby coefficients in thresholding or subtraction step. We propose using the dip map data structure to connect local curvelet coefficients together in the noise attenuation process. In the specific case of multiple subtraction, matching and subtraction of curvelet coefficient independently can lead to primary damage. We avoid this problem by using estimated dip maps for the primary and multiple components to guide the adaptation process. Our example on real dataset shows that the improved multiple subtraction algorithm removes more residual multiples while preserving primaries.

Acknowledgements

We would like to thank PGS for permission to publish, and our colleagues, R. Dyer, S. Perrier, L. Marsiglio, P. Lecocq and S. Brandwood for reviewing this paper.

References

- Neelamani, R et al. [2008] Coherent and random noise attenuation using the curvelet transform, The Leading Edge, Feb. 2008 pp.240-248
- Neelamani, R. et al. [2010] Adaptive subtraction using complex-valued curvelet transforms Geophysics (2010),75(4):V51
- Nguyen, T. and Dyer, R. [2016] Adaptive multiple subtraction by statistical curvelet matching, SEG Technical Program Expanded Abstracts 2016: pp. 4566-4571.
- Nguyen, T. and Chauris, H. [2010] The Uniform Discrete Curvelet Transform IEEE Transactions on Signal Processing 08/2010; 58(7):3618 - 3634.
- Perrier, S., Dyer, R., Liu, Y.J. Nguyen, T. and Lecocq, P., [2017] Intelligent adaptive subtraction for multiple attenuation, EAGE 2017.

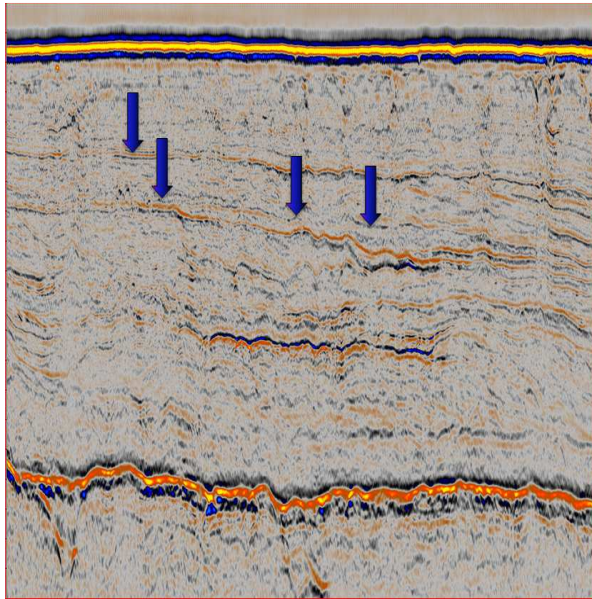


Figure 3: Stack of the multiple denoising results in channel domain using conventional simultaneously Least-Squares Filtering based adaptive subtraction.

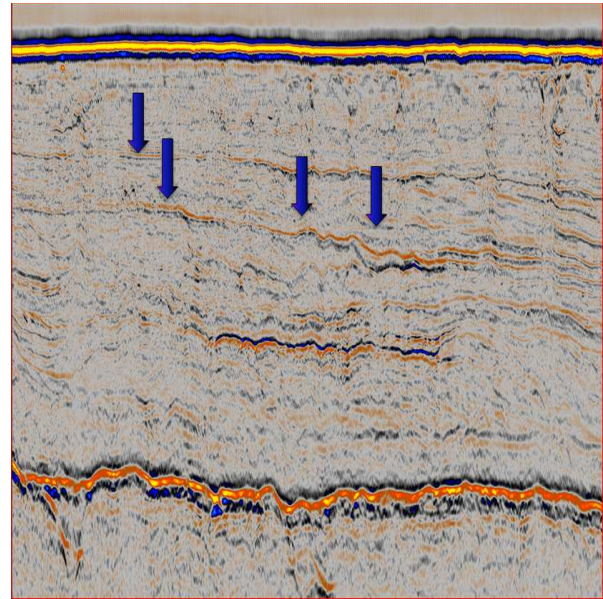


Figure 4: Stack of the multiple attenuation result after applying this newly improved method in channel domain with a running window of 1000 traces in the space direction.

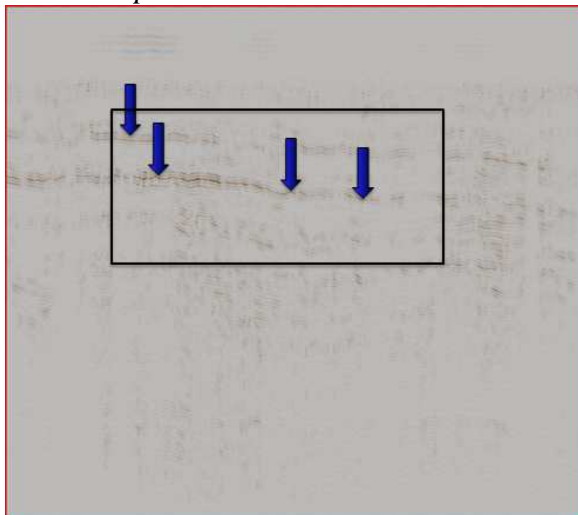


Figure 5: Stack result difference (scaled by 2) This demonstrates clearly that primaries are well preserved while more multiples are attenuated.

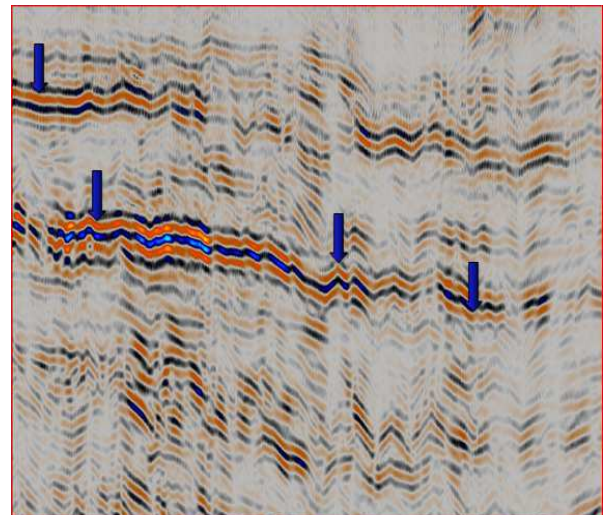


Figure 6: Stack result difference in the boxed area in Figure 5 (scaled by 10).